J. Am. Chem. Soc. 1991, 113, 855-861

XPS Studies of Solvated Metal Atom Dispersed Catalysts. Evidence for Layered Cobalt-Manganese Particles on Alumina and Silica

Beng Jit Tan, Kenneth J. Klabunde,* and Peter M. A. Sherwood*

Contribution from the Department of Chemistry, Willard Hall, Kansas State University, Manhattan, Kansas 66506. *Received September 29, 1989, Revised Manuscript Received June 12, 1990*

Abstract: XPS studies of solvated metal atom dispersed (SMAD) catalysts coupled with detailed studies of reference compounds were carried out. It was shown that toluene-solvated cobalt atoms nucleate at surface OH groups, and the resultant cobalt oxide surface species serve as sites for nucleation of more cobalt atoms, leading to very small, reactive metallic clusters. The surface of these clusters/particles are partially oxidized by adventitious oxygen or water, but when cobalt loadings of over 4% are used, a major portion of the catalytic particle remains metallic. When solvated cobalt and manganese atoms are mixed together, the manganese atoms deposit first at surface OH sites, and manganese is highly dispersed in this way, but the majority ends up as surface MnO and Mn_2O_3. Some of the deposited manganese atoms/clusters serve as nucleation sites for cobalt atoms. In this way a layered catalytic particle is formed: support (SiO_2 or Al_2O_3) covered by manganese oxide which in turn is covered by metallic cobalt. The manganese material serves as a gradient between the ionic support oxide and metallic cobalt, and the composite is quite stable and highly active in catalysis. Also, the manganese serves as a sacrificial metal, serving to scavenge oxidizing moieties (mostly OH groups) on the support surface, thereby allowing cobalt to deposit and remain metallic and very highly dispersed. Sizes of the composite particles are probably 10-30 Å in diameter and are nearly amorphous.

Introduction

By preparing solvated metal atoms, systems that generally have limited thermal stability, we have discovered a convenient way of preparing very highly dispersed metallic catalysts on various supports.[1-9] In this procedure the solvated atom solutions are exposed to high surface area supports at low temperature, for example, in liquid toluene at -96 °C. As the resultant slurries warm, the metal atom solvates slowly decompose and deposit metal atoms on the support surface:

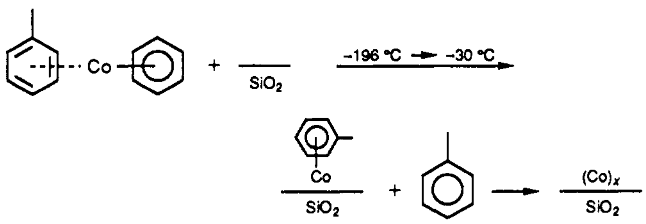

As more and more atoms deposit, very small metal clusters are formed under mild conditions, and the catalysts thus prepared are catalytically ready and do not require reduction steps or other pretreatment steps.

The catalytic activities of SMAD catalysts invariably are very high,[7,8] and stabilities and lifetimes are also quite good, so further work on these new materials seems warranted.

In earlier work on Co/SiO_2 and $Co-Mn/SiO_2$ bimetallic system, we found (1) 60% dispersion of Co without Mn, but >90% when Mn was included,[8] (2) EXAFS studies suggested that Mn was in an oxidized state on a SiO_2 surface where much of the Co was in a metallic state.[9] In fact, the Mn behaved as a sacrificial metal scavenging oxidizing sites on the SiO_2, enabling the Co to remain metallic. (3) Ensemble effects of Mn on Co particles did not appear to be important.[8] These results, combined with the intriguing catalytic activities of the Co-Mn systems, encouraged us to carry out investigations further.

When dealing with a homogeneous solution of two sensitive, reactive metal atom solvates, which are simultaneously exposed to a high surface area support, a natural question is "which metal atom solvate will decompose on the support surface first, and on what sites?" Little is known about the necessary chemical properties of a nucleation site on a SiO_2 or Al_2O_3 surface. Surface area definitely has an effect on resultant metal particle size, and the number of acidic sites also appears to be important.[5,10] However, predicting whether $(sol)_xMn$ or $(sol)_xCo$ would deposit/nucleate first is virtually impossible. All these considerations prompted us to carry out the study reported herein, an XPS study of SMAD Co/support and SMAD Co-Mn/support catalysts. Based on these data and those of our earlier work, we can now propose a unique model for these supported bimetallic particles.

Experimental Section

Materials. Metals were obtained in high-purity forms from Matheson, Coleman and Bell (Mn) and Cerac, Inc. (Co). The catalyst supports used were American Cyanamid γ-alumina (200 m^2/g) and Davison silica (300 m^2/g). These supports were calcined at 500 °C for 3 h in flowing dry air (420 mL/min) and cooled in flowing nitrogen (500 mL/min). Toluene was used exclusively as the metal atom codeposition solvent and was purified according to methods described earlier.[5] High-purity commercially available (Alfa Products) metals, oxides, and hydroxides were used as reference materials.

Catalyst Preparations. The metal vapor SMAD method has been described earlier.[4,5,7,8,11,12] Metal loadings (weight %) are quoted in the text. All samples were prepared under vacuum and then removed from the reactor under pure N_2.

XPS Experiments. X-ray photoelectron spectra were obtained by using an AEI ES200B spectrometer with Mg X-radiation ($h\nu$ = 1253.6 eV). The power was 240 W (12 kV and 20 mA), and the vacuum of the

---

(1) Klabunde, K. J.; Efner, H. F.; Satek, L.; Donley, W. J. *J. Organomet. Chem.* **1974**, *71*, 309.

(2) Klabunde, K. J.; Efner, H. F.; Murdock, T. D.; Ropple, R. *J. Am. Chem. Soc.* **1976**, *98*, 1021.

(3) Klabunde, K. J.; Ralston, D. H.; Zoellner, R.; Hattori, H.; Tanaka, Y. *J. Catal.* **1978**, *55*, 213.

(4) Matsuo, K.; Klabunde, K. J. *J. Catal.* **1982**, *73*, 216.

(5) Klabunde, K. J.; Tanaka, Y. *J. Mol. Catal.* **1983**, *21*, 57 and references therein.

(6) Kanai, H.; Tan, B. J.; Klabunde, K. J. *Langmuir* **1986**, *2*, 760.

(7) Klabunde, K. J.; Imizu, Y. *J. Am. Chem. Soc.* **1984**, *106*, 2721.

(8) Imizu, Y.; Klabunde, K. J. In *Catalysts of Organic Reactions*; Augustine, R. L., Ed.; Marcel Dekker: New York, 1985.

(9) Tan, B. J.; Klabunde, K. J.; Tanaka, T.; Kanai, H.; Yoshida, S. *J. Am. Chem. Soc.* **1988**, *110*, 5951.

(10) Matsuo, K.; Klabunde, K. J. *J. Org. Chem.* **1982**, *47*, 843.

(11) Li, Y. X.; Klabunde, K. J. *Langmuir* **1987**, *3*, 558.

(12) Description of metal vapor chemistry techniques in general: Klabunde, K. J.; Timms, P. L.; Skell, P. S.; Ittel, S. *Inorg. Syn.* **1979**, *19*, 59.

0002-7863/91/1513-855$02.50/0

Table I. XPS Binding Energies (eV) for Cobalt Reference Compounds[a]

	Co $2p_{3/2}$			Co $2p_{1/2}$						Co $2p(2p_{1/2} + 2p_{3/2})$/O 1s[b]	
sample	MP	SS	ΔS	MP	SS	ΔS	Δ	Al 2p	O 1s		
Co metal	777.3			792.4			15.1				
Co_3O_4	779.6	787.1	7.5	794.8	804.1	9.3	15.2		529.3	530.7	0.60 (0.75)
CoO	780.1	788.0	7.9	795.3	804.6	9.3	15.2		529.8	531.6	0.53 (1.00)
$Co(OH)_2$	781.0	786.4	5.4	796.9	802.6	5.7	15.9		531.2		0.25 (0.50)
Co_2O_3	780.2	786.5	6.3	796.0	803.7	7.7	15.8		530.1	531.6	0.42 (0.67)
Al_2O_3								74.5	531.4		

[a] MP = binding energy of the main peak, SS = binding energy of satellite peak, ΔS = energy separation between the main peak and satellite peak, and Δ = spin–orbit splitting; error limits are ±0.2 eV. [b] Figures in parentheses indicate the theoretical atomic ratio based upon anhydrous materials.

sample chamber was in the range of 10^{-8} to 10^{-9} Torr. The spectrometer was operated in the fixed analyzer transmission (FAT) mode with a pass energy of 65 eV. The reference compounds and SMAD catalysts were mounted onto the sample probe with the aid of Scotch-brand double-sided sticky tape.

Preparations of samples for XPS studies were carried out in an argon-filled inert atmosphere box (Vacuum Atmospheres). The catalysts, in dry powder form, were dusted onto the sample block covered with double-sided sticky tape. The sample block was built so that it could be retracted into a sealable sample probe and sealed using a gold O-ring. (This sealable sample probe was designed after that reported by Hercules and co-workers,[13] and allowed transfer of the sample under completely inert atmosphere conditions.) An outer chamber was screwed onto the probe so as to keep the entire probe in an inert environment before removing it from the inert atmosphere box. The probe was then transferred to the XPS instrument. The outer chamber was removed before inserting the probe into the insertion lock of the spectrometer. The insertion lock was then evacuated and the probe was transferred into the main chamber. Once in the main chamber, the sample block was opened slowly to expose the sample. The sample chamber was pumped down until the vacuum reached 10^{-8} Torr and the X-ray gun was then switched on.

Data were collected using an Apple II microcomputer and transferred to an IBM PC/AT for data analysis. Binding energies of the reference compounds and catalysts were measured using the C 1s peak (284.6 eV) of the adventitious carbon as an internal standard. Argon ion etching was performed with a saddle field Ion-Tech B22 ion gun.

XPS intensity ratios were determined using the total integrated areas of the Mn 2p, Co 2p, O 1s, and Al 2p photoelectron lines. Peak area computation was performed after a nonlinear background was removed.[14a] Spectra were fitted using a nonlinear least-squares program with a mixed Gaussian–Lorentzian product function.[14c] Difference spectra and normalization was performed using our previously described method.[14] The atomic ratios were calculated taking into account the Scofield photoelectron cross sections,[15] and differences in inelastic near free path (assuming imfp $\propto \sqrt{KE}$). An infinite thickness, uniform composition sample was assumed in calculating atomic ratios.

Results

Cobalt Reference Compounds. Binding energies of the Co 2p and O 1s regions are given for Co metal, CoO, Co_3O_4, and $Co(OH)_2$ in Table I. The Co 2p line positions for the reference compounds are sufficiently chemically shifted to allow easy identification. For example, the Co $2p_{3/2}$ line for $Co(OH)_2$ was chemically shifted 1.4 eV to higher binding energy than for Co_3O_4. The Co 2p photoelectron spectrum of the CoO sample resembled that of Co_3O_4 initially. This is because the surface of CoO is readily oxidized to Co_3O_4 in air. After the sample was argon ion etched for 5 min, the main 2p peaks broadened and shifted to higher binding energy, and intense satellite peaks appeared. The spectral features were then similar to those reported by Kim[16] and Pollack[17] for CoO (surface Co_3O_4 had been sputtered away). It should be noted that Co_3O_4 is stable in air at room temperature.[18] This is in contrast to Fe_3O_4 and Mn_3O_4 where their surfaces readily oxidize to Fe_2O_3 and Mn_2O_3.[19]

Table II. XPS Binding Energies (eV) for Manganese Reference Compounds

compound	Mn $2p_{3/2}$[a]	Mn $2p_{1/2}$[a]	Δ[b]	O 1s	Mn $2p(2p_{1/2} + 2p_{3/2})$/O 1s[c]
MnO_2	641.9 (3.4)	653.6 (3.5)	11.7	529.2	0.29 (0.50)
Mn_3O_4	641.3 (3.2)	652.9 (3.3)	11.6	529.1	0.48 (0.75)
MnO	641.4 (3.6)	653.1 (3.9)	11.7	529.8	0.53 (1.00)
Mn_2O_3	641.7 (3.2)	653.4 (4.0)	11.7	529.8	0.46 (0.67)
Mn	638.6 (1.9)	649.7 (2.5)			

[a] Peak widths full width at half-maximum (fwhm) are listed in parentheses. [b] Δ = spin–orbit splitting. [c] Figures in parentheses on the right-hand column indicate the theoretical atomic ratios based upon anhydrous materials.

The Co_3O_4 has a spinel structure and contains magnetic Co^{2+} ions in the A-sites (tetrahedral sites) and diamagnetic Co^{3+} ions in the B-sites (octahedral sites). These two sites are indistinguishable by XPS. Although all compounds containing high-spin Co^{2+} ions have strong satellite peaks in Co 2p spectra,[20] Co_3O_4 only has weak satellites in this region. These satellites occur about 7–9 eV higher in binding energy from the main bands, which agree well with literature reports.[19] High-spin Co^{2+} core level spectra (as in CoO) show strong satellite peaks above the main 2p lines. Frost and co-workers[19,21] have shown that high-spin Co^{2+} compounds exhibit intense satellites while low-spin Co^{2+} compounds either exhibit weak or missing satellites in their photoelectron spectra. Thus, it is not difficult to differentiate high-spin Co^{2+} compounds from Co_2O_3. Cobalt hydroxide has a strong satellite peak associated with both the lines of the Co2p region. Satellite peaks in these reference compounds have been attributed to shake up excitation.[22,23]

The O 1s spectrum of each of these oxides consists of two peaks around 531 and 529 eV. The first is due to hydroxide and/or absorbed water, while the second is due to the oxide lattice ions; these values agree well with those reported earlier.[20,23]

Manganese Reference Compounds. Table II summarizes XPS data for Mn, MnO, and MnO_2, Mn_2O_3, and Mn_3O_4 in the O 1s and Mn 2p regions. Our values agree very well with earlier data of Carver and co-workers.[24] The binding energies of Mn $2p_{3/2}$ and Mn $2p_{1/2}$ for the oxides lie within a narrow range, which

---

(13) (a) Ng, K. T.; Hercules, D. M. *J. Phys. Chem.* **1976**, *80*, 2094. (b) Patterson, T. A.; Carver, J. C.; Leyden, D. E.; Hercules, D. M. *J. Phys. Chem.* **1976**, *80*, 1700.

(14) (a) Proctor, A.; Sherwood, P. M. A. *Anal. Chem.* **1980**, *52*, 2315. (b) Proctor, A.; Sherwood, P. M. A. *Anal. Chem.* **1982**, *54*, 13. (c) Sherwood, P. M. A. In *Practical Surface Analysis by Auger and X-ray Photoelectron Spectroscopy*; Briggs, D., Seah, M. P., Eds.; Wiley: New York, 1983, Appendix 3.

(15) Scofield, J. H. *J. Electron Spectrosc. Relat. Phenom.* **1976**, *8*, 129.

(16) Kim, K. S. *Phys. Rev. B* **1975**, *11*, 2177.

(17) Pollak, R. A. Ph.D. Thesis, Lawrence Berkeley Laboratory Report LBL-1299, 1972.

(18) Kubashewski, O.; Evans, E. L.; Alcock, C. B. *Metallurgical Thermochemistry*, 4th ed.; Sangyo Tosho: Tokyo, 1968.

(19) Frost, D. C.; McDowell, C. A.; Woolsey, I. S. *Mol. Phys.* **1974**, *27*, 1473.

(20) Chuang, T. J.; Brundle, C. R.; Rice, D. W. *Surf. Sci.* **1976**, *59*, 413.

(21) Frost, D. C.; McDowell, C. A.; Woosley, I. S. *Chem. Phys. Lett.* **1972**, *17*, 320.

(22) Carlson, T. A.; Cawer, J. C.; Saethre, L. F.; Garua Santibanez, F.; Vernon, G. A. *J. Electron Spectrosc. Relat. Phenom.* **1974**, *5*, 247.

(23) McIntrye, N. S.; Cook, M. G. *Anal. Chem.* **1975**, *47*, 1975.

(24) Carver, J. C.; Schweitzer, G. K. *J. Chem. Phys.* **1972**, *57*, 973.

Table III. XPS Parameters (eV)[a] for Unsupported SMAD Co Catalysts

	Co $2p_{3/2}$			Co $2p_{1/2}$				O 1s[b]	
treatment	MP	SS	ΔS	MP	SS	ΔS	Δ		
fresh	780.8	785.9	5.1	796.7	802.5	5.8	15.9	531.5	529.8
etched (2 min)	777.3, 780.8	785.9	5.1	792.4, 796.7	802.5	5.8	15.1, 15.9	531.5	529.8

[a] MP = binding energy of main peak. SS = binding energy of satellite peak. ΔS = energy separation between satellite peak and main peak. Δ = spin–orbit splitting. [b] The peak at highest binding energy is substantially reduced in intensity on etching.

Table IV. XPS Parameters (eV)[a] for SMAD Co/Al_2O_3 Catalysts

	Co $2p_{3/2}$			Co $2p_{1/2}$				O 1s		
catalysts	MP	SS	ΔS	MP	SS	Δs	Δ			Al 2p
1.6% Co	780.5	785.7	4.9	796.1	801.8	5.7	15.6	531.4 (2.9)	529.5 (2.9)	74.0 (3.3)
3.8% Co	780.9	786.1	5.2	796.5	802.3	5.8	15.6	531.4 (2.9)	529.6 (2.9)	74.5 (2.6)
8.2% Co	780.3	785.3	5.0	795.9	801.9	6.0	15.6	531.4 (2.9)	529.6 (2.9)	74.2 (2.8)
11.0% Co	781.2	786.4	5.2	797.0	803.0	6.0	15.8	531.2 (2.9)	529.6 (2.9)	74.9 (2.8)
12.3% Co	780.7	785.7	5.0	796.4	802.6	6.2	15.7	531.4 (2.9)	529.6 (2.9)	74.7 (2.7)

[a] Symbols have the same meaning as in Table I.

Table V. XPS Peak Area Intensity Ratios for SMAD Co/Al_2O_3 Catalysts

catalyst	Co 2p/Al 2p	Co 2p/O 1s	Al 2p/O 1s	(CoO + Al_2O_3)/ $Co(OH)_2$	CoO/ $Co(OH)_2$	%Al_2O_3 in O 1s peak
1.6% Co	0.13	0.08	0.63	4.2	1.1	56
3.8% Co	0.37	0.19	0.50	3.9	2.4	32
8.2% Co	0.52	0.23	0.43	2.2	1.1	27
11.0% Co	0.43	0.23	0.53	2.4	0.95	36
12.3% Co	0.48	0.21	0.45	2.4	1.2	31

Table VI. XPS Binding Energies (eV)[a] for SMAD 3.2% Co–4.0% Mn/SiO_2 Catalyst

	Co $2p_{3/2}$		Co $2p_{3/2}$		O 1s		
treatment	MP	SS	MP	SS			Si 2p
fresh	780.4	785.6	796.3	802.0	531.4	529.6	102.3 (2.6)
etched	777.7, 780.8		792.8, 796.9		531.4	529.6	
air exposed	780.5	786.1	796.0	802.0	531.4	529.6	103.6

[a] Peak widths (fwhm) are listed in parentheses. MP = binding energy of the main peak; SS = binding energy of the satellite.

caused difficulty in unambiguous identification in our catalyst samples.

SMAD Catalysts. (a) Unsupported Cobalt SMAD Catalysts. Table III summarizes the electron binding energies of the Co 2p and O 1s regions of a freshly prepared unsupported Co SMAD catalyst before and after a 2-min argon ion etch (see Figure 1 which shows the Co 2p region).

Comparing the Co 2p binding energies, satellites, and line shapes with reference compounds, the surface of the fresh sample appeared to be mainly $Co(OH)_2$. After the etch, the Co $2p_{3/2}$ envelope consisted of a sharp peak corresponding to cobalt metal and a shoulder at 780.8 eV corresponding to a mixture of Co(II) hydroxide and Co(II) oxide. Satellite peaks associated with the Co 2p main line for Co^{2+} were also observed.

Spectral subtraction was performed on the spectrum of the etched sample by subtracting from it a weighted fraction of the spectrum of the fresh sample (see Figure 1c), which yielded spectral features very similar to those found for cobalt metal foil (Co 2p region), although somewhat broader.

The O 1s envelope of the fresh SMAD sample showed peaks at 529.8 and 531.5 eV corresponding to oxide and hydroxide species (possibly adsorbed water as well). Etching caused the loss of some hydroxide and adsorbed water, and the intensity of the 531.5 peak decreased. There was also an increase in the Co 2p/O 1s intensity ratio from 0.4 to 1.0 after etching.

(b) Unsupported Manganese SMAD Catalysts. The Mn 2p photoelectron peaks from the unsupported Mn SMAD catalyst before and after etching are shown in Figure 2. The Mn $2p_{3/2}/2p_{1/2}$ binding energies for the fresh sample were found at 640.8/652.5 eV (with Mn $2p_{3/2}$ satellite separation of 11.7 eV), which are similar to those for MnO (641.4 and 653.1) and Mn_2O_3 (641.7/653.4). This suggests that the surface species are a mixture of MnO and Mn_2O_3. Before etching, a shoulder at even higher binding energy from the Mn$2p_{3/2}$ peak was noted, which became more prominent after etching. This shoulder could be attributed to a shake-up satellite characteristic of Mn^{2+}.

Table VII. Peak Area Intensity Ratios for SMAD 3.2% Co–4.0% Mn/SiO_2 Catalysts As They Undergo Various Treatments

sample	Mn $2p_{3/2}$/ Si 2p	Mn $2p_{3/2}$/ Co $2p_{3/2}$	Mn 2p/ O 1s	Co $2p_{3/2}$/ Mn $2p_{3/2}$
fresh	0.092	0.67	0.048	1.5
etched	0.077	0.92	0.043	1.1
air exposed	0.13	0.88	0.069	1.1

The fwhm decreased when the sample was etched and the Mn $2p_{3/2}/2p_{1/2}$ core level photoelectron peaks shifted slightly to lower binding energy (640.5/652.2). The Mn $2p_{3/2}$/O 1s intensity ratio rose from 0.4 to 0.6 on etching.

(c) SMAD Co/Al_2O_3 Catalysts. The Co 2p core level photoelectron peaks of a few examples of SMAD Co/Al_2O_3 were examined with a nonlinear background removed. Very noticeable feature of all the spectra were the intense satellite peaks (see Table IV). By comparing these spectra with the reference compounds, it can be concluded that the surface species are a mixture of mainly cobalt(II) hydroxide and some cobalt(II) oxide. No evidence for cobalt aluminate was found. The Al 2p peak for the Al_2O_3 support was found at 74.5 eV.

Table VIII. XPS Parameters (eV)[a] for SMAD Co–Mn/Al_2O_3 Catalysts

	Co $2p_{3/2}$			Co $2p_{1/2}$			
catalyst	MP	SS	ΔS	MP	SS	ΔS	Δ
5.1% Co–4.6% Mn	780.6	785.6	5.0	796.3	801.9	5.6	15.7
4.3% Co–3.0% Mn	780.4	785.8	5.4	796.2	802.2	6.0	15.8
6.9% Co–1.5% Mn	780.2	785.7	5.5	796.0	802.5	6.5	15.8

[a] MP = binding energy of the main peak, SS = binding energy of the satellite peak, ΔS = energy separation of the satellite peak from the main peak, and Δ = spin–orbit splitting.

Table IX. Co 2p XPS Parameters (eV)[a] for SMAD Co–Mn/Al_2O_3 Catalysts after a 5-min Argon Ion Etch

	Co $2p_{3/2}$				Co $2p_{1/2}$					
catalyst	MP		SS	ΔS	MP		SS	ΔS	Δ	
5.1% Co–4.6% Mn	777.9	780.4	785.4	5.0	793.0	796.1	802.4	6.3	15.1	15.7
6.9% Co–1.5% Mn	777.9	780.5	785.5	5.0	792.9	796.2	802.4	6.2	15.0	15.7

[a] Binding energies referenced to C 1s = 284.6 eV. MP = binding energy of the main peak, SS = binding energy of the satellite peak, ΔS = energy separation of the satellite peak from the main peak, and Δ = spin–orbit splitting.

Table X. Normalized Co 2p Peak Area Intensities of the Difference Spectra for Co–Mn Catalysts

sample	normalized area
3.2% Co–4.0% Mn/SiO_2	565
5.1% Co–4.6% Mn/Al_2O_3	601
6.9% Co–1.5% Mn/Al_2O_3	780

The O 1s envelope consisted of two peaks at 531.4 and 529.5 eV, corresponding to $Co(OH)_2$ and CoO plus Al_2O_3, respectively.

Table V summarizes the area ratios of the Co 2p, O 1s, and Al 2p peaks for the SMAD catalysts. The O 1s peaks can be fitted to one peak corresponding to CoO and Al_2O_3 and one peak due to $Co(OH)_2$; hence the ratio of (CoO + Al_2O_3)/$Co(OH)_2$ can be evaluated. While CoO and Al_2O_3 cannot be distinguished by binding energy difference, the Al 2p/O 1s area ratio in pure Al_2O_3 can be used together with the Al 2p area to ascertain how much of the signal corresponding to (CoO + Al_2O_3) corresponds to CoO; this is listed in Table V. The Co 2p/O 1s ratio showed a sharp increase in going from loadings of 1.6% Co to 3.8% Co, and leveled off with further increase in cobalt loading. Similar results were found for the Co 2p/Al 2p ratio.

(d) SMAD Co–Mn Supported Catalysts. Figure 3 shows the Co 2p photoelectron spectra for a fresh sample of 3.2% Co–4.0% Mn/SiO_2 catalyst, after etching, and after exposing the etched sample to air at ambient conditions for 5 min (a nonlinear background was removed).

Table VI summarizes the Co 2p and O 1s data while Table VII summarizes the changes in peak area intensity ratios as the catalyst underwent these treatments. The spectral features, particularly the strong satellite bands, indicate that the surface species are a mixture of CoO and some $Co(OH)_2$.

The Si 2p photoelectron peak for SiO_2 was observed at 102–103 eV. Our XPS results do not indicate the presence of cobalt silicate.

The 3-min etch resulted in the appearance of the cobalt metal peak. There was a shoulder on the higher energy side of this peak which could be attributed to a mixture of CoO and $Co(OH)_2$. On exposure to air, the spectrum for $Co(OH)_2$ was reobtained (see Figure 3).

Figure 4 illustrates what happened to the Mn 2p region with the etch and then air exposure. The fresh sample appears to consist of MnO and Mn_2O_3 surface species. Upon etching the Mn 2p peak shifted slightly to lower binding energy with little change in the Mn 2p/O 1s ratio (Table VII). Air exposure caused an increase in this ratio and shifted the Mn 2p peak to higher binding energy again. These results indicate that the manganese may not be fully oxidized, but is nearly so, in this SMAD catalyst.

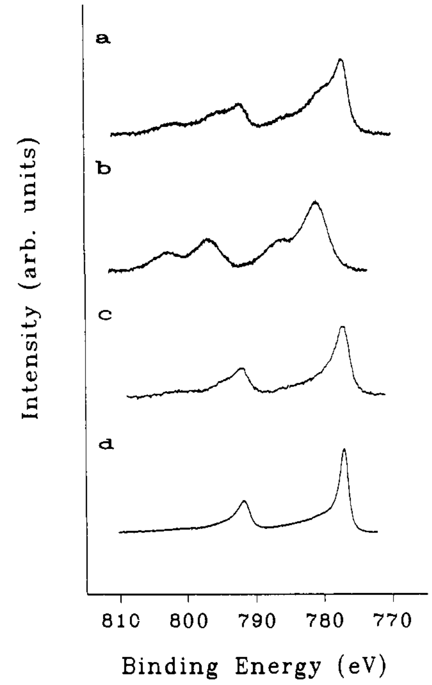

Figure 1. Co 2p XPS spectra of unsupported SMAD cobalt catalyst: (a) after a 2-min argon etch, (b) fresh sample, (c) difference spectrum obtained by subtracting (b) from (a), and (d) cobalt metal.

We now turn our attention to the XPS results for the Co–Mn/Al_2O_3 catalysts. The Co 2p, Mn 2p, and O 1s peaks of the fresh and etched samples resembled those for the SiO_2 supported system (Tables VIII and IX). The binding energies for the fresh sample suggest a mixture of $Co(OH)_2$ and CoO on the surface. A 2-min etch revealed metallic cobalt. The spectrum of the fresh sample was substracted from that of the etched sample to obtain the difference spectrum. The area under the difference spectrum was normalized by dividing the peak area by the total number of spectral scans. Since the instrument settings (scan rate, period, and scan width) were the same for all the spectra collected, the area per scan would also be the peak area per unit time of spectral collection. These data are summarized in Table X. The normalized area increased with cobalt loading, which verifies the expected result that increased loading gives a higher ratio of metallic cobalt in the core of the catalyst particles. Furthermore, Table XI lists the peak area intensity ratio, and, as expected, the

Table XI. XPS Peak Area Intensity Ratios for SMAD Co–Mn/Al_2O_3 Catalysts

	fresh			etched (5 min)		
catalyst	Co 2p/Al 2p	Co 2p/Mn 2p	Mn 2p/Al 2p	Co 2p/Al 2p	Co 2p/Mn 2p	Mn 2p/Al 2p
5.1% Co–4.6% Mn/Al_2O_3	0.22	1.7	0.13	0.13	1.2	0.11
6.9% Co–1.5% Mn/Al_2O_3		3.5		0.43	2.5	0.17

Table XII. Mn 2p XPS Parameters[a] for Supported SMAD Co–Mn Catalysts

	fresh					etched (5 min)				
catalyst	Mn $2p_{3/2}$	Mn $2p_{3/2}$	Δ	O 1s		Mn $2p_{3/2}$	Mn $2p_{3/2}$	Δ	O 1s	
6.9% Co–1.5% Mn/Al_2O_3	641.2	653.0	11.8	531.4 (2.7)	529.7 (2.7)	641.0	652.7	11.7	531.4 (2.7)	529.7 (2.7)
5.1% Co–4.6% Mn/Al_2O_3	640.7	652.5	11.8	531.4 (2.8)	529.7 (2.8)	640.6	652.3	11.7	531.4 (2.8)	529.7 (2.8)
3.2% Co–4.0% Mn/SiO_2	640.7	652.6	11.9	531.4 (2.6)	529.7 (2.6)	640.6	652	11.7	531.4 (2.6)	529.7 (2.6)

[a] Peak width (fwhm) listed in parentheses. Δ = spin–orbit splitting.

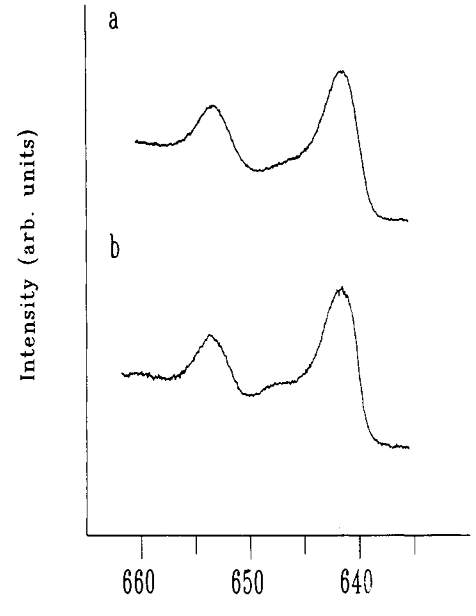

Figure 2. Mn 2p XPS spectra of unsupported SMAD manganese catalyst; (a) fresh sample and (b) after a 90-s argon ion etch.

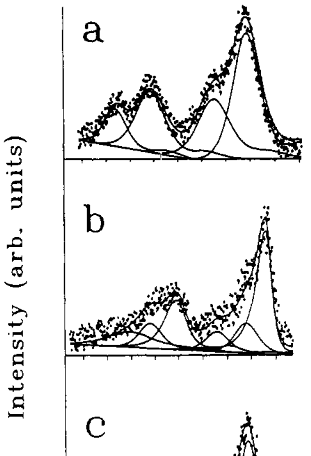

Figure 3. Co 2p XPS spectra of SMAD 3.2% Co–4.0% Mn/SiO_2 catalyst with nonlinear background removed: (a) fresh sample, (b) after a 3-min argon ion etch, and (c) oxidized in air for 5 min. All peaks were fitted to a 50% Gaussian/Lorentsian mix except for the metal peaks in (6) which used an 80% mix. Weak features to high binding energy of component peaks are due to X-ray satellites.

Co 2p/Al 2p ratio increased with cobalt loading (see data on etched sample).

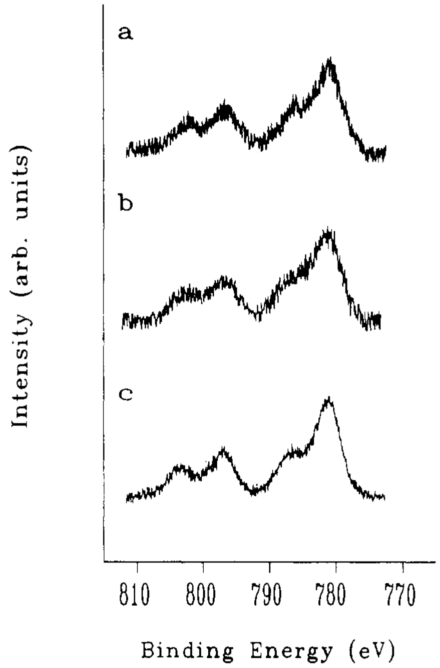

Figure 4. Mn 2p XPS spectra of SMAD 3.2% Co–4.0% Mn/SiO_2 catalyst: (a) fresh sample, (b) after a 3 min argon ion etch, and (c) oxidized in air for 5 min.

The binding energy of the Mn 2p peaks for both SiO_2 and Al_2O_3 supported catalysts lie slightly lower than those for MnO and Mn_2O_3. The etched samples showed the characteristic shake-up satellites for Mn^{2+}. These results (Table XII) indicate that manganese was mainly in an oxidized state, with perhaps a small amount of nonfully oxidized manganese present.

Discussion

The work with reference compounds and unsupported cobalt and manganese SMAD catalysts allowed confirmation of several points: (1) unsupported Co SMAD particles consist of metallic cobalt cores incorporating some carbonaceous material; (2) in spite of airless handling methods, thin surface layers of $Co(OH)_2$ were present, probably from scavenging of trace amounts of water and/or oxygen. Etching revealed some CoO but also metallic cobalt. Using the argon ion gun of the ES200B instrument, a short 2--3-min etch time will remove about 10–20 Å of impurities, mainly adventitious carbonaceous species, on the surface of the particles.[25] (Longer etch times will certainly reduce the oxides and hydroxides, eventually giving the metal. Thus, we examined the etching of standard CoO and $Co(OH)_2$ samples and did observe reduction, especially after >5-min etch times. There is thus some possibility that the etching caused some reduction, but with the short etch times it does not appear significant in the present context.) With removal of such an overlayer, it becomes possible to detect photoelectrons deeper into the metallic clusters. Thus, after etching, the metallic peak increased substantially. The

---

[25] Breeze, P. A.; Hartnagel, H. L.; Sherwood, P. M. A. *J. Electrochem. Soc.* **1980**, *127*, 454.

etching experiments suggest that the unsupported particles consist of metallic cobalt covered with a very thin layer of CoO, then $Co(OH)_2$, and an easily removed carbonaceous layer on the surface.

Etching also removed other adventitious species such as adsorbed molecular oxygen and water, which resulted in a decrease in the intensity of the O 1s peak and an increase in the Co 2p/O 1s ratio.

For the unsupported Mn SMAD particles, only oxidized species were observed. Etching did not reveal metallic manganese. Thus, even though the bulk of the sample is metallic (it is pyrophoric), scavenging of oxidizing moieties is so efficient that rather thick layers of metal oxide are present.

Supported SMAD catalysts, with high surface area supports, invariably have been shown to consist of very small metallic particles, essentially amorphous, probably in the 10–30-Å size range.[5,9,10] Such particles should be highly susceptible to oxidation by trace water or O_2, and by support hydroxyl groups or oxophobic defect sites. Hence, our XPS results for low loading of Co on Al_2O_3 showed that the Co 2p/O 1s ratio was low, suggesting metal oxide and hydroxide surface coatings. On increasing the cobalt loadings, metallic cobalt became observable (after etching). In addition, for studies of samples with change in cobalt loading, the Co 2p/O 1s ratio increased as the percent of cobalt went up, and then leveled off after a 4 wt% loading was reached (these experiments were without etching). This suggests that, after about a 4 wt % cobalt loading, no more Al_2O_3 was being covered up by cobalt by increasing the cobalt loading (see Table V). This in turn suggests that nucleation sites were exhausted after a 4% loading was reached. From then on, as cobalt loading increased, particle growth was the result.

Other data that bear on this point deal with the Co 2p/Al 2p intensity area ratio (for Co/Al_2O_3 SMAD catalysts). We observed an initial increase in this ratio up to 8% Co/Al_2O_3 which then leveled off with increasing cobalt loadings. This result also suggests that between 4% and 8% loading all of the nucleation sites are exhausted.

It is interesting to compare the number of surface OH groups available with the amount of cobalt (as atoms) available. Taking five surface OH groups/nm² using 200 m²/g of Al_2O_3, there are 1×10^{21} OH groups/g, or 1.7×10^{-3} mol/g.[26] Cobalt, at a 3.8% loading by weight would be 0.69×10^{-3} g-atom. So approximately two OH groups would be available/Co atom, which would be the necessary number stoichiometrically

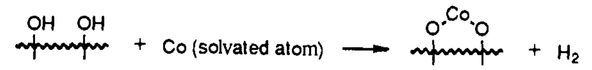

to oxidize the cobalt atom. Thus, above a 4% cobalt loading, the OH groups should be all scavenged and nucleation of metallic cobalt would become more favored:

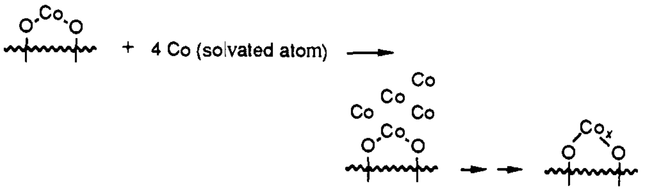

Actually this calculation supports our findings for Co 2p/Al 2p ratio changes surprisingly well. Once more than a 4% cobalt loading is reached, when more cobalt is available, apparently no more new particles form, existing particles grow, and so XPS scanning of an area of surface should reveal little change in Co/Al ratio.

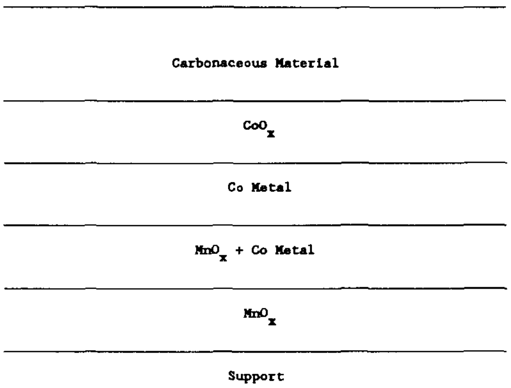

Figure 5. Catalyst model for supported SMAD Co–Mn system. This is an XPS view of the surface with the surface composition averaged over a relatively large area. The layer just above the support is richer in manganese oxide. Cobalt is present as a surface hydroxide/oxide in the surface and inner layer just above the support and a metallic middle layer.

With regard to the Co 2p/O 1s ratio, where about 4% cobalt loadings were needed in order to stabilize the Co/O ratio, this may be due to the need to buildup a thick cobalt particle before O 1s diminishes. A very thin layer of cobalt, ligated by surface oxygen, would still allow the observation of O1s under the thin layer of cobalt,

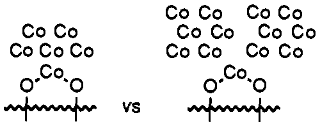

Thus, we can rationalize our XPS intensity ratios based on the idea that surface OH groups serve as nucleation sites for formation of Co SMAD catalyst particles.

Co–Mn Supported SMAD Catalysts. Surface species on both the SiO_2- and Al_2O_3-supported bimetallic catalysts were found to be cobalt hydroxide and manganese(II) oxide and manganese(III) oxide. Light argon ion etching allowed more MnO to be observed at the expense of Mn_2O_3. Exposure of the etched sample to air reestablished the Mn_2O_3 intensity. For cobalt, etching allowed enhanced intensity for CoO and the observation of metallic cobalt (which became the major peak; see Figure 3).

Interestingly, the Co 2p/Mn 2p ratios for catalysts that had comparable loadings of Co and Mn (Table VIII, 3.2% Co–4.0% Mn/SiO_2; Table XI, 5.1% Co–4.6% Mn/Al_2O_3) were found to be higher according to XPS than would be predicted based on the amounts of metal amployed. Thus, Co/Mn ratios are 0.80 (predicted) and 1.5 (found) and 1.1 (predicted) and 1.7 (found) for these two catalysts. This point suggests that cobalt resides nearer the surface of the particle and is covering some of the manganese. In addition, the Co 2p/Mn 2p ratio decreased on etching, again supporting this layering idea. This result agrees with our earlier data on chemisorption and catalytic data,[8,9] and deserves further discussion.

Manganese is more oxophilic than cobalt. Also, toluene-solvated Mn atoms are less thermally stable toward aggregation than toluene-solvated cobalt atoms. These considerations would lead to the prediction, based on our earlier discussion of cobalt particle formation on surface OH sites, that manganese atoms may react with surface OH groups before cobalt atoms. In such a way nucleation sites rich in manganese may be formed that could serve as "friendly" sites for subsequent cobalt nucleation/deposition. In fact, our earlier EXAFS work suggested this.[9] Furthermore, about a 3–4% Mn loading was required so that all the cobalt observed by EXAFS was in the metallic state.[9]

On the other hand, closer evaluation of the data suggests that when very low loadings on Mn are employed, the surface is not totally covered by cobalt. Note that for the low Mn loading (Table XI; 6.9% Co–1.5% Mn/Al_2O_3) the Co/Mn ratio is 4.6 (predicted) and 3.5 (found). It would appear that, in a case like this, the large amount of cobalt present overwhelms the manganese, and perhaps cobalt nucleates and forms particles of its own accord in addition to in concert with manganese. Indeed, catalytic data show that

---

(26) Boehm, H. P. *Adv. Catal.* **1966**, *16*, 249.

Scheme I

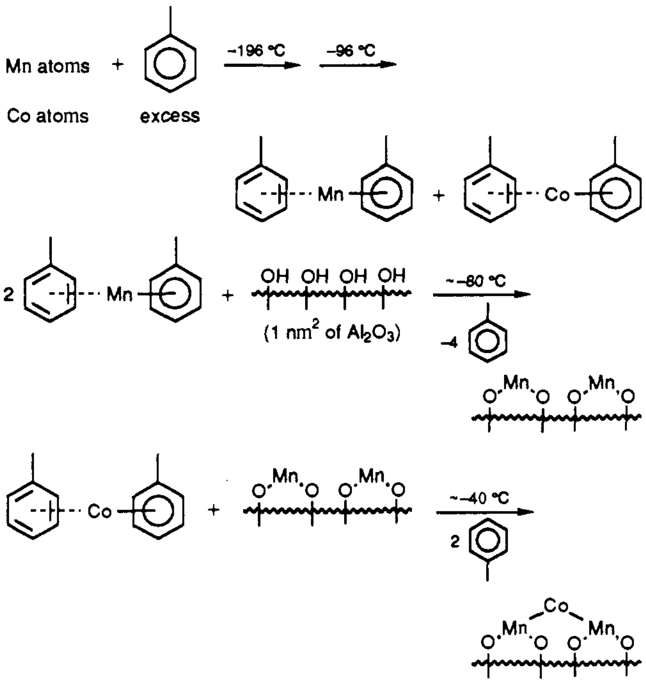

these low loadings of Mn are not as effective as loadings that are close to 1:1 Co to Mn.[8,9]

Another interesting point is that in the Co–Mn/Al_2O_3 catalysts the Co/Al ratio is slightly higher than the Mn/Al ratio (Table XI). This suggests that the cobalt is covering a significant portion of the manganese. Also, although the manganese is probably spread more widely than cobalt, still significant amounts of uncovered Al_2O_3 exist.

Structures of the Co–Mn Supported Catalyst Particles. All of these data combined with our previous results can be best explained by the sequence shown in Scheme I, which is oversimplified and ignores adsorbed surface O_2, H_2O, and carbonaceous material. Figure 5 illustrates a more realistic layered structure that is actually observed by XPS.

The important thing to note is the formation of manganese oxide on the support surface. In this way the manganese serves as a sacrificial metal and allows metallic cobalt to deposit on it and remain metallic. This sequencing also serves to give a gradation from ionic oxide (support) to a partially oxidized nonstoichiometric oxide (MnOx) to a metallic material (Co metal), a "graded-seal"[27] type of anchoring to the support. This may explain the good thermal and catalytic stability of these bimetallic materials.

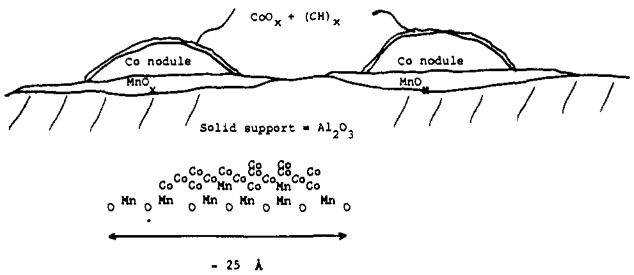

Figure 6. Idealized bimetallic Co–Mn/Al_2O_3 particles in two dimensions. The upper figure shows the generalized view, and the lower figure more detail of a cobalt nodule/particle.

What a cutaway (side view) of a catalyst particle may look is shown in an oversimplified way in Figure 6, which again ignores adsorbed O_2, H_2O, and carbonaceous material. The size of the particle is shown to be about 25 Å in diameter which is in accord with our earlier EXAFS, XRD, and chemisorption studies.

Conclusions Regarding Co–Mn/Supported SMAD Catalysts

(1) The manganese serves as a sacrificial metal, scavenging oxidizing surface OH groups as well as trace amounts of adventitious oxygen and water. In doing so it becomes oxidized to MnO and Mn_2O_3.

(2) A higher portion of manganese deposits on the support surface first, and some of the deposited Mn atoms/clusters serve as nucleation sites for cobalt atoms.

(3) Cobalt is protected from substantial oxidation by the presence of sufficient amounts of manganese.[9]

(4) The catalyst particle formed with a gradation of ionic oxide (support) to partially oxidized nonstoichiometric oxide (MnOx) to metallic cobalt. This "graded-seal" type of particle strongly adheres to the support surface.

(5) No prereduction step, as is common practice with conventionally prepared catalysts, is required in order to activate the SMAD catalyst.[7,8] Thus, small amounts of $Co(OH)_2$ or CoO that are formed on the active metallic cobalt surface are apparently readily removed during catalytic reactions.

(6) These are new catalytic materials, and the concept of a sacrificial metal for aid in forming such unique support/oxide/metal gradiated particles is promising for further new material syntheses.

Acknowledgment. The support of the National Science Foundation is acknowledged with gratitude. We also thank Drs. George Lester, Hiroyoshi Kanai, Tsunehiro Tanaka, and Professor Satohiro Yoshida for helpful discussions.

---

(27) Dr. George Lester first introduced this term to us, in reference to catalysts.